CRACK GROWTH MODELLING: ENRICHED CONTINUUM VS. DISCRETE MODELS

Vinh Phu Nguyen[1,*], Giang Dinh Nguyen[1], Daniel Dias-da-Costa[2], Luming Shen[2], Chi Thanh Nguyen[1]
[1]School of Civil, Environmental & Mining Engineering,
The University of Adelaide, Adelaide, SA 5005, Australia
*Email: phu.nguyen@adelaide.edu.au
[2]School of Civil Engineering, The University of Sydney, NSW 2006, Australia.

ABSTRACT

Failure in quasi-brittle materials usually appears in the form of narrow bands called fracture process zones, where all inelastic deformation takes place, while the surrounding bulk material outside those areas typically unloads elastically. This localised nature of failure is the main source of size effects in these materials, since the width of the fracture process zone is a material property that does not scale with the size of the material volume. An adequate description of localised failure and associated size effects requires both size and behaviour of the fracture process zone and neighbouring material to be properly taken into account. In this study, we present two alternative approaches for modelling localised failure and simulating fracture propagation using finite element methods. In the first approach, an embedded crack appears at a constitutive level by enriching the kinematics of constitutive models, while in the second one this is done at the finite element level using cohesive interface elements. The advantages and shortcomings of both are presented through one numerical example on the failure of fibre-reinforced composite materials.

KEYWORDS

Quasi-brittle, cohesive crack, constitutive modelling, finite elements, interface elements.

INTRODUCTION

Localised mode of failure is usually encountered in quasi-brittle materials such as concrete, rock and ceramics. The deformation in such cases usually localises on narrow bands where all inelastic deformation takes place and the surrounding bulk material outside those areas typically unloads elastically. Since the width and orientation of the localisation band are both material properties, taking them into account in constitutive modelling of quasi-brittle materials is critical for a correct description of their post-localisation behaviour. This behaviour in such cases, scales with the width of the localisation band and the size of the volume element that contains it. This is the well-known 'size effect' mentioned in the literature.

Localised failures have traditionally been modelled using two approaches - the continuous and the discontinuous approach. Notable models belong to the former class include nonlocal constitutive models (Bazant and and Pijaudier-Cabot 1988), gradient enhanced damage models (Peerlings *et al*. 1996), smeared crack models (Rashid 1968, Bazant and Oh 1983), and recently emerged phase field models (Miehe *et al*. 2010). The key characteristics of the continuous approach is that the failure process is modelled by the degradation of the material and therefore the incorporation of a length scale is done at the constitutive level, or alternatively at the integration point level in a numerical method framework, such as the finite element method (FEM). Its name reflects one of the drawbacks of the continuous approach - true separation cannot be captured since the continuum, even though cracked, is always simulated as continuous medium. This is due to the fact that cracks are not explicitly represented; only their effects are taken into account through the degradation of effective properties of the continuum. On the other hand, discontinuous approaches employ explicit crack representations and hence allow material separation to be accurately reproduced as a geometrical discontinuity. Some of the methods for localised failure include zero-thickness cohesive interface elements (Ngo and Scordelis 1968, Xu and Needleman 1994, Mergheim *et al*. 2004, Dias-da-Costa *et al*. 2009a, Nguyen 2014a), elements with embedded strong discontinuities (Dvorkin *et al*. 1990, Dias-da-Costa *et al*. 2009b, 2013) and extended finite elements (XFEM) (Moes *et al*. 1999, Wells and Sluys 2001). Cohesive zone models (Barenblatt 1962 and Dugdale 1960) are usually employed in discontinuous approaches.

In this paper a comparison of computational performances, particularly the efficiency and robustness, of the continuous approach and the discontinuous approach is established for the modelling of quasi-brittle failure. We use the kinematically enriched constitutive model developed recently by (Nguyen *et al*. 2012, 2014, 2015b) as a

continuous approach. For the discontinuous approach, the cohesive interface elements are used in the framework of discontinuous Galerkin approach recently employed by Nguyen (2015a). These two different approaches are used in the simulation of a fibre-reinforced composite material at the mesoscale, where both matrix and fibres are explicitly represented. All simulations are carried out on the same computer using the same FE solver facilitating the comparison of these approaches. In the next section, the kinematically enriched constitutive model approach is presented, followed by the formulation of a cohesive element in Section 3. In the last sections, the numerical example and findings are discussed and conclusions withdrawn.

KINEMATICALLY ENRICHED CONSTITUTIVE MODEL

General case

We consider a material volume Ω consisting of a localisation zone Ω_i of thickness h, surrounded by a bulk material Ω_O (Fig. 1). Subscripts "i" and "o" are used for quantities inside and outside the localisation band, respectively (Einstein summation convention does not apply here). Accordingly, the stresses and strains are denoted by $(\boldsymbol{\sigma_i}, \boldsymbol{\epsilon_i})$, $(\boldsymbol{\sigma_o}, \boldsymbol{\epsilon_o})$ for the material inside and outside the localisation band, the latter within the homogeneous bulk. Dissipative processes are assumed to take place exclusively inside the thin localisation band, while the outside bulk is undergoing elastic unloading. Note that this assumption belongs to a more general case of discontinuous bifurcation, and while it is valid for quasi-brittle materials such as concrete, it may not hold for other materials. Examples of these materials include the ones with inelastic unloading outside shear bands such as in granular materials. The point is to devise a model, in terms of the averaged (or macro) stress $\boldsymbol{\sigma}$ and averaged strain $\boldsymbol{\epsilon}$ defined over the domain Ω, by coupling the different responses of the material inside and outside the localised region i.e., in terms of $(\boldsymbol{\sigma_i}, \boldsymbol{\epsilon_i})$, $(\boldsymbol{\sigma_o}, \boldsymbol{\epsilon_o})$, η, h and H (definitions shown in Fig. 1).

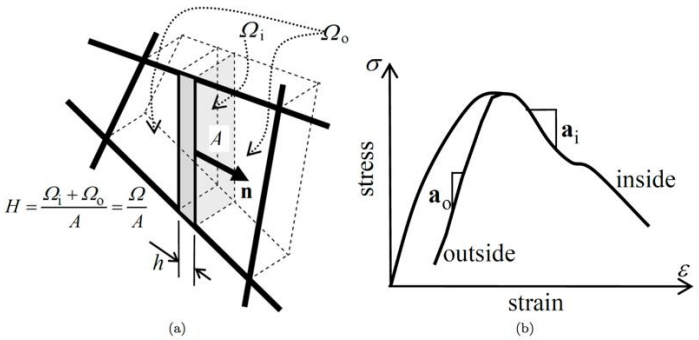

Figure 1: Numerical discretisation and a localisation zone (shadowed) (a) and corresponding material responses inside and outside the localisation zone (b) (after Nguyen et al., 2014).

Key-equations are presented here, while further details can be found in (Nguyen *et al*. 2012, 2014, 2015b). The macro strain rate is defined as the volume-averaged strain rates inside and outside the localisation band:

$$\dot{\boldsymbol{\epsilon}} = \eta\dot{\boldsymbol{\epsilon}}_i + (1-\eta)\dot{\boldsymbol{\epsilon}}_o \tag{1}$$

where η is the volume fraction of the localisation band, $\eta = \frac{h}{H}$ (Fig. 1). Given a very narrow localisation band, usually approximated by a zero thickness cohesive zone in quasi-brittle failure, the strain rate inside the localisation band can be approximated as

$$\boldsymbol{\epsilon}_i \approx \frac{1}{h}\,(\boldsymbol{n} \otimes [\![\dot{\boldsymbol{u}}]\!])^{sym} \tag{2}$$

where $\boldsymbol{n}$ denotes the outward unit vector normal to the localisation band and $[\![\dot{\boldsymbol{u}}]\!]$ is the velocity jump vector. One can see Equations (1-2) as a kinematic enrichment at the constitutive level due to the appearance of an additional strain rate in the constitutive description. This enrichment allows for the introduction of an additional constitutive behaviour for the material inside the localisation band. We can write the behaviour inside and outside the band in generic forms as:

$$\boldsymbol{\sigma}_o = \boldsymbol{a}_o : \dot{\boldsymbol{\epsilon}}_o,\ \dot{\boldsymbol{\sigma}}_\iota = \boldsymbol{a}_i : \dot{\boldsymbol{\epsilon}}_i \tag{3}$$

where $\boldsymbol{a}_o$and $\boldsymbol{a}_i$ are the fourth-order material tangents of the materials outside and inside, respectively.

The connection between inside/outside quantities with the homogenised ones is enforced via the Hill-Mandel equation that should be met for any arbitrary strain rate $\dot{\boldsymbol{\epsilon}}$ and velocity jump $[\![\dot{\boldsymbol{u}}]\!]$:

$$\boldsymbol{\sigma}:\dot{\boldsymbol{\epsilon}} = \eta\boldsymbol{\sigma}_i:\dot{\boldsymbol{\epsilon}}_i + (1-\eta)\boldsymbol{\sigma}_o:\dot{\boldsymbol{\epsilon}}_o \tag{4}$$

Using (1-4), it can be shown that (i) the macro homogenised stress $\boldsymbol{\sigma}$ coincides with the stress $\boldsymbol{\sigma}_o$ describing the behaviour of the material outside the localisation zone, and (ii) the traction must be continuous across the boundary of the localisation zone:

$$\boldsymbol{\sigma} = \boldsymbol{\sigma}_o \text{ and } \boldsymbol{\sigma_i}\cdot\boldsymbol{n} = \boldsymbol{\sigma_o}\cdot\boldsymbol{n} \tag{5}$$

The above traction continuity condition – together with Equations (1-3) – is the key to determine the velocity jump vector from a given macro strain rate $\dot{\boldsymbol{\epsilon}}$. Ignoring the details – these can be found in Nguyen *et al* (2014) – we can write:

$$[\![\dot{\boldsymbol{u}}]\!] = \left[\frac{\eta}{h}\boldsymbol{A}_o + \frac{1-\eta}{h}\boldsymbol{A}_i\right]^{-1}\cdot(\boldsymbol{a}_o:\dot{\boldsymbol{\epsilon}})\cdot\boldsymbol{n} = \boldsymbol{C}^{-1}\cdot\ (\boldsymbol{a}_o:\dot{\boldsymbol{\epsilon}})\cdot\boldsymbol{n} \tag{6}$$

where $\boldsymbol{C}$ is the tensor in the square brackets; $\boldsymbol{A}_o$and $\boldsymbol{A}_i$ are the acoustic tensors associated with $\boldsymbol{a}_o$and $\boldsymbol{a}_i$, respectively, $\boldsymbol{A}_{o/i} = \boldsymbol{n}\cdot\boldsymbol{a}_{o/i}\cdot\boldsymbol{n}$. From (1-3 and 5), the stress strain relationship, in rate form, can be obtained as

$$\dot{\boldsymbol{\sigma}} = \frac{1}{1-\eta}\boldsymbol{a}_o:\left[\dot{\boldsymbol{\epsilon}} - \frac{\eta}{h}(\boldsymbol{n}\otimes(\boldsymbol{C}^{-1}\cdot(\boldsymbol{a}_o:\dot{\boldsymbol{\epsilon}})\cdot\boldsymbol{n}))^{sym}\right] \tag{7}$$

Note that the second term in the above expression accounts for cracking effects by a relaxation strain rate governed by the behaviour inside the localisation zone. In other words, cracking is modelled as a material degradation process in the same manner as damage models or smeared crack models. However, unlike these existing approaches that lump everything in a single macro constitutive behaviour, the key difference here is the separation of constitutive responses inside and outside the localisation zone, and the utilisation of their connection via the traction continuity to constitute macro homogenised behaviour. Since cracking is dealt with at the constitutive level, or at the integration points in a FEM context, there is no need to enhance the element interpolation functions, and hence all element technology remains the standard one. This is the key-advantage of the continuous approach relatively to discontinuous formulations, which depend on the type of element.

The aforementioned constitutive model has been firstly used with a plastic-damage model to describe the localisation band, whereas the region outside this band was assumed to be linear elastic (Nguyen *et al*. 2014). It was then used in (Nguyen *et al*. 2015a) to model shear bands in geomaterials. In the next section, the specialisation of this general constitutive model to the case in which the localisation band can be modelled as a cohesive crack is presented.

Embedded cohesive cracks

Cohesive crack models adopt a traction-separation law instead of the stress-strain law usually used for the bulk. In a local coordinate system aligned with the crack, the cohesive law generally reads:

$$\boldsymbol{t}_{cr} = \boldsymbol{K}_{cr}[\![\dot{\boldsymbol{u}}]\!]_{cr} \tag{8}$$

where subscript '*cr*' is used to indicate that the cohesive law is defined in the crack coordinate system. The traction vector is denoted by $\boldsymbol{t}_{cr}$ and $\boldsymbol{K}_{cr}$ is the second-order cohesive material tangent.

In the case of cohesive cracks, the localisation band is simply a surface/line in three/two dimensions corresponding to $h \to 0$. Using $f = h/H$, Equations (1, 2) can be simplified into

$$\dot{\boldsymbol{\epsilon}} = \frac{1}{H}\ (\boldsymbol{n}\otimes[\![\dot{\boldsymbol{u}}]\!])^{sym} + \dot{\boldsymbol{\epsilon}}_o \tag{9}$$

The velocity jump given in Equation (5) then becomes

$$[\![\dot{\boldsymbol{u}}]\!] = \left[\frac{1}{H}\boldsymbol{A}_o + \boldsymbol{K}\right]^{-1} \cdot (\boldsymbol{a}_o : \dot{\boldsymbol{\epsilon}}) \cdot \boldsymbol{n} \tag{10}$$

where $\boldsymbol{K}$ denotes the cohesive material tangent defined in the global coordinate system. In the same manner, the stress-strain relationship is now given by

$$\dot{\boldsymbol{\sigma}} = \boldsymbol{a}_o : \left[\dot{\boldsymbol{\epsilon}} - \frac{1}{H}(\boldsymbol{n} \otimes (\boldsymbol{C}^{-1} \cdot (\boldsymbol{a}_o : \dot{\boldsymbol{\epsilon}}) \cdot \boldsymbol{n}))^{sym}\right] \tag{11}$$

where $\boldsymbol{C}$ is the tensor defined by $\boldsymbol{C} = \frac{1}{H}\boldsymbol{A}_o + \boldsymbol{K}$ (the term in square brackets in Equation (10)).

Advantages of the enriched constitutive model

The preliminary works of (Nguyen et al, 2012, 2014, 2015ab) on kinematically enriched constitutive models showed several advantages. In particular, and similarly to any continuum approach, when compared to discontinuous methods such as XFEM, the enriched constitutive modelling approach is robust and efficient (e.g. no additional unknowns are required such as with XFEM). It can be easily implemented in existing mesh-based or particle-based numerical codes (even in some commercial packages, since only a constitutive routine is needed) and able to handle crack branching, intersecting and merging. This is particularly interesting in the case of large-scale simulations involving complex cracking processes, where the discrete representation of cracks might not be feasible and the smeared crack approach limits the element size, which may not be satisfied due to the typical element sizes (in the order of meters). Current practice to solve this issue relies on artificially increasing the fracture energy or reducing the tensile strength (Levy *et al*. 2011). In this sense, compared to existing smeared crack models, the enriched approach is free of the so-called local snapback instability, which settles the limit on the finite element size for the standard smeared crack approach. The use of two inter-dependent constitutive relationships for bulk and localisation zone, and their corresponding sizes, together with a two-level stress return algorithm (Nguyen *et al*., 2015b), naturally resolves snap-back issues and gives the model an intrinsic scaling law to deal with size effects.

DISCRETE CRACK MODELLING

Among various discrete crack modelling techniques (cohesive interface elements, XFEM, embedded strong discontinuities, among others) the zero-thickness cohesive interface elements are herein adopted due to the (i) robustness, (ii) easy implementation (even for parallel computers) and (iii) ability to model complex crack patterns, see for example (Xu and Needleman 1994, Nguyen 2014a). These interface elements are inserted into the mesh prior to the simulation using the tool developed by (Nguyen 2014b), cf. Fig. 2, within the framework of a discontinuous Galerkin method. It should be emphasised that cohesive interface elements are to some extent mesh-dependent since the crack path is constrained to the element edges/surfaces, although this is not pronounced for complex crack patterns as shown in (Nguyen 2014b).

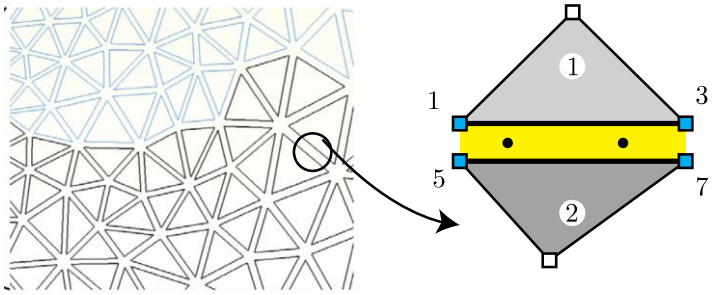

Figure 2: Zero-thickness interface elements embedded in a mesh of triangles (left) and a typical four-node linear interface element (nodes are 1, 3, 5, 7) (right).

The weak form is the standard one-field variational formulation given as follows

$$\int_\Omega \delta\boldsymbol{u} \cdot \boldsymbol{b} d\Omega + \int_{\Gamma_t} \delta\boldsymbol{u} \cdot \bar{\boldsymbol{t}}\, d\Gamma = \int_\Omega \delta\boldsymbol{\epsilon} : \boldsymbol{\sigma}(\boldsymbol{u}) d\Omega + \int_{\Gamma_d} \delta[\![\boldsymbol{u}]\!] \cdot \boldsymbol{t}^c([\![\boldsymbol{u}]\!])\, d\Gamma \tag{11}$$

where Ω is the domain of interest, Γ_t denotes the traction boundary, Γ_d is the crack surfaces (which constitute all the element edges in two dimensions and element surfaces in three dimensions), $\boldsymbol{b}$ is the body force, $\bar{\boldsymbol{t}}$ is the applied traction, $[\![\boldsymbol{u}]\!]$ is the displacement jump (that measures the crack separation) and $\boldsymbol{t}^c$denotes the cohesive traction. Note that only the last term in Equation (11), which is work done by the cohesive cracks, differs from the standard weak form. In this approach, conventional interface elements are used in conjunction with the so-called intrinsic cohesive law (cf. Figure 3-left). In this case, the initial elastic stiffness of the interface elements artificially increases the compliance of the system. One solution to this issue is to employ an initially rigid cohesive law (cf. Fig. 3-right) together with a discontinuous Galerkin (dG) formulation (Mergheim *et al* 2004) to link the solid elements before crack initiation. Details on the dG cohesive interface elements, computer implementation and applications can be found in (Nguyen 2014a).

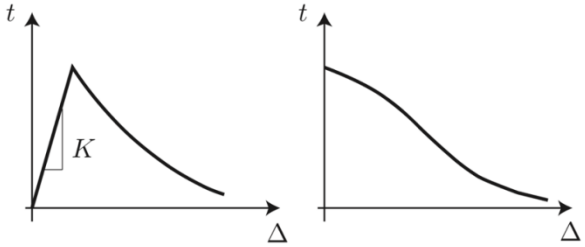

Figure 3: Two types of cohesive laws: intrinsic cohesive law or initially elastic one (left) and extrinsic or initially rigid cohesive law (right).

RESULTS AND DISCUSSIONS

This section presents some simulations of the failure of a fibre-reinforced composite sample shown in Fig. 4. Note that this sample was selected just for illustration and comparison of two approaches and it is probably not representative of a real composite material. The material properties are the following: Young's modulus and Poisson's ratio of the matrix, 4 GPa and 0.4, respectively, Young's modulus and Poisson's ratio of the fibres are 40 GPa and 0.33, respectively. For matrix cracks, a tensile strength of 30 MPa is adopted with a fracture energy of 0.25 N/mm, whereas for the interfacial cracks, the tensile strength is 10 MPa and the fracture energy is 0.05 N/mm. As can be seen, the nonlinearities are assumed to originate from cracking solely and the bulk is modelled as linear elastic.

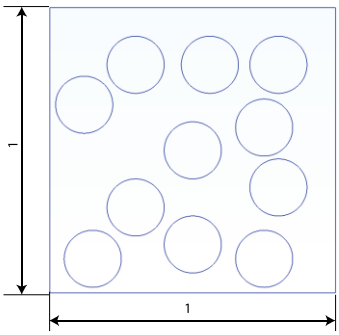

Figure 4: A unit square made of fibre-reinforced composite material. All fibres are represented by circles of the same radius of 0.1 mm. A uniaxial tensile test is performed where the left edge is fixed in both directions and the right edge is pulled horizontally. Plane stress condition is assumed.

The discretisation of the domain in Fig. 4 consists of 15680 linear triangular elements (7909 nodes), and on that discretisation basis, modifications to fit the requirements of continuous and discontinuous approaches are needed. Only a single discretisation basis is considered since the mesh objectivity of the continuous approach was already demonstrated elsewhere (Nguyen *et al*. 2012, 2014), while the discontinuous one intrinsically has dissipation scaling with surface areas and hence is free from zero dissipation modes when the element size goes to zero. In this study, for both approaches, matrix-fibre debonding is explicitly modelled using cohesive elements and this is obtained by inserting interface elements only at the matrix/fibre interface. For the discontinuous approach, a further modification is needed by inserting interface elements at every element boundaries except for elements discretising the fibres, since the fibres are assumed elastic. The continuous approach in this case employs 15680 solid elements and 616 interface elements with a total of 8525 nodes (mesh 1), while the finite element mesh for continuous approach contains 15680 solid elements and 12744 interface elements with a total of 28999 nodes (mesh 2, which has three times the number of nodes compared to mesh 1). For further details, the first mesh is used with standard cohesive elements to model matrix/fibre debonding and

the kinematically enriched constitutive model (at the integration points of the bulk elements) to model the matrix cracking. The second mesh is used with standard cohesive elements to model matrix/fibre debonding and with dG cohesive elements to model the matrix cracking.

As for the cohesive laws, the model developed by (Turon *et al*. 2006), which is a mixed-mode initially elastic bilinear cohesive law[1], is adopted. The simulations are carried out using a displacement control and the nonlinear equations are solved using a full standard Newton-Raphson method. Figure 5 shows the crack patterns obtained with the two approaches. It should be noted that modelling the matrix/fibre debonding requires a discontinuous approach (i.e. interface elements). If a continuous approach is to be used, then a thin layer around the fibres is needed (Nguyen *et al*. 2010). Finding the thickness of this thin layer is not trivial and its meshing can result in many elements. For this reason, interface elements were selected for modelling debonding.

As can be observed, similar crack patterns are obtained using both formulations. In terms of the load-displacement response (measured at the right edge), as shown in Fig. 6, there is a small discrepancy between the two approaches. The discontinuous response is more brittle than the continuous response, this difference is more pronounced at later stages of the failure process. This is expected since it is well known that continuous approaches cannot accurately capture the kinematics of strong geometrical discontinuities: in Fig. 5 true separation of the matrix phase can be obtained by the dG cohesive elements, whereas cracks are represented by widely stretched elements in the continuous approach. In the continuous approach, crack orientation is locally determined from the first principle stress at the integration point and is not restricted to a predefined orientation dictated by the element boundaries, as with cohesive interface elements. However, as noted in (Wells and Sluys, 2001), the use of a nonlocal stress field for retrieving the orientation of the crack can avoid stress-locking effects and the more ductile behaviour observed with the continuous approach could be a result of such locking. Further investigations are still needed.

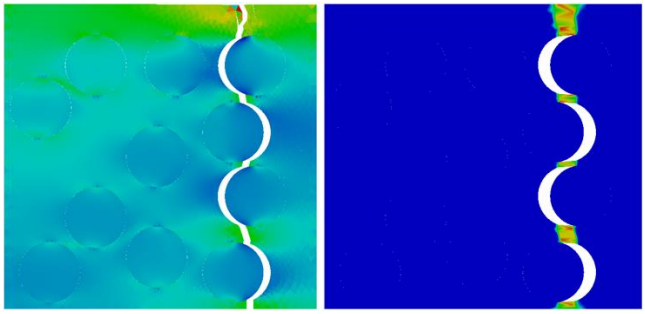

Figure 5: Crack patterns obtained with the discontinuous approach (left) and the combined continuous-discontinuous approach (right). Colour in the left denotes the stress field (σ_{xx}) and the colour in the right figure represents the damage field.

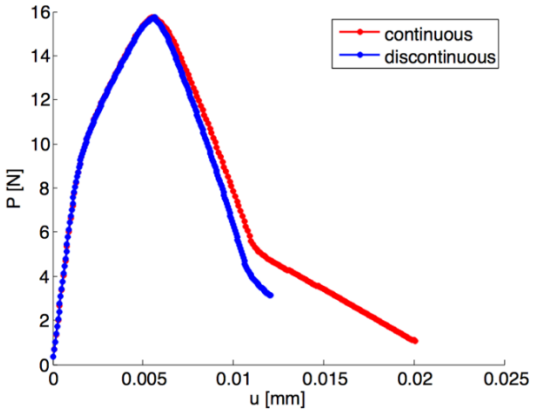

Figure 6: Response in terms of load-displacement curves. After an initial elastic regime, the debonding of the matrix/fibre interface resulted in a nonlinear hardening response with a reduced stiffness. At the peak, a dominant crack has propagated through the sample. A softening post-peak response is observed with the opening of this dominant crack.

[1] From this initially elastic cohesive law, an initially rigid cohesive law can be straightforwardly obtained by 'shifting'. Details can be found in (Nguyen 2014a).

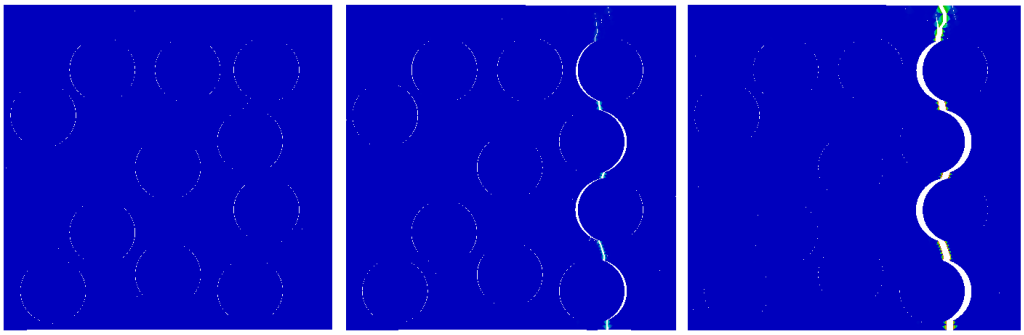

Figure 7: Cracking process of fibre-reinforced composite materials starts with interface debonding and the coalescence of the cracks into a dominant crack that runs through the sample.

The cracking process of fibre-reinforced composite materials, depicted in Fig. 7[2], starts with interface debonding (interfacial cracks) and then cracks tend to kink into the matrix, before finally coalescing into a dominant crack running through the sample. During later stages the other cracks close. This is qualitatively in good agreement with experimental observations by París *et al*. (2006), example shown in Fig. 8.

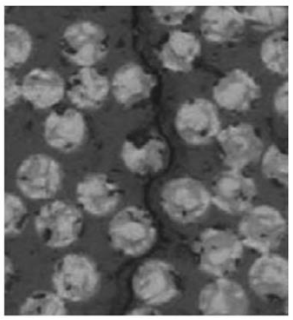

Figure 8: Failure of fibre-reinforced composite materials from experiments (París et al. 2006).

DISCUSSION AND CONCLUSIONS

In terms of computational cost and robustness, the continuous approach performs better than the discontinuous approach, thanks to its design that does not need any other element enrichments that may introduce additional degrees of freedom to the system. As a consequence, the simulation using the enriched constitutive model for the matrix cracking ran in about 360 seconds while the one using dG cohesive interface elements took about 2790 seconds, which is approximately 7 times slower. Note that this is not only due to a higher number of nodes (28999 nodes compared with 8525 nodes) but also due to the fact that the dG cohesive elements suffered from convergence issues with large increments, and hence small displacement increments (half of those used in the continuous approach) were needed. The discontinuous approach could, however, be optimised such that the interface elements would be introduced in the region of interest, thus reducing the number of degrees of freedom. Advanced solution-finding techniques such as non-iterative solution methods, see (Graça-e-Costa et al. 2012) and references therein, and viscous regularisation techniques can also be used to improve the robustness of the discontinuous analyses.

The proposed continuous approach however suffers from the well known stress locking issue when elements with multiple integration points are used. The use of linear triangle elements in the presented example does inhibits the stress locking issues due to the fact that only a single integration point in the element is used to capture the effect of a single crack within the element. In this sense, the orientation of the crack crossing the element is correctly represented by a single cohesive crack at the constitutive (or integration point) level (Fig. 1). However, when elements with multiple integration points (for example quadrilateral elements or quadratic triangle elements) are used, the elements contain several cohesive cracks, each one with its own orientation. This is a source of severe stress locking, as experienced by Nguyen *et al*. (2014) as the separation of the element into two parts cannot be guaranteed. Therefore, a simple resolution is to base the determination of crack orientations at all integration points in an element on a nonlocal stress field and enforce the same orientation for

[2] Animation of these simulations can be found at
https://www.youtube.com/watch?v=QPb_vqUlx7o&feature=youtu.be.

all cracks in the element. Alternatively transition from constitutive enrichment to element based enrichment (Dias-da-Costa *et al*., 2009, 2013) is also expected to alleviate this locking effect. These issues and corresponding resolutions will be addressed in our future work.

ACKNOWLEDGMENTS

Funding support from the Australian Research Council via projects DP140100945 (Luming Shen, Giang D. Nguyen, Vinh Phu Nguyen), DE150101703 & FCOMP-01-0124-FEDER-020275/ PTDC/ECM/119214/2010 (Daniel Dias-da-Costa) and FT140100408 (Giang D. Nguyen) is gratefully acknowledged.

REFERENCES

Barenblatt, G. (1962). "The mathematical theory of equilibrium cracks in brittle fracture". *Advanced Applied Mechanics* 7, 55–129.

Bazant, Z. and Oh, B. (1983). "Crack band theory for fracture in concrete". *Materials and Structures* 16 155–177.

Bazant, Z. and Pijaudier-Cabot, G. (1988). "Nonlocal continuum damage, localization instabilities and convergence". *Journal of Engineering Mechanics* (55) 287–293.

Dias-da-Costa, D., Alfaiate, J., Sluys, L. J. and Júlio, E. (2009a). "A comparative study on the modelling of discontinuous fracture by means of enriched nodal and element techniques and interface elements". *International Journal of Fracture* 161(1) 97 – 119.

Dias-da-Costa, D., Alfaiate, J., Sluys, L. J., and Julio E. (2009b). "A discrete strong discontinuity approach". *Engineering Fracture Mechanics* 76 (9) 1176 – 1201.

Dias-da-Costa, D., Alfaiate, J., Sluys, L. J., Areias, P., Júlio, E. (2013). "An embedded formulation with conforming finite elements to capture strong discontinuities". *International Journal for Numerical Methods in Engineering* 93 (2) 224–244.

Dugdale, D. (1960). "Yielding of steel sheets containing slits". *Journal of the Mechanics and Physics of Solids* 8(2), 100–104.

Dvorkin, E.N., Cuitino, A. M. and Gioia G. (1990). "Finite elements with displacement interpolated embedded localization lines insensitive to mesh size and distortions". *International Journal for Numerical Methods in Engineering* 30 541–564.

Graça-e-Costa, R., Alfaiate, J., Dias-da-costa, D., Sluys, L.J. (2012). "A non-iterative approach for the modelling of quasi-brittle materials". *International Journal of Fracture* 178:281– 298.

Levy, G. Coon, M., Nguyen, G.D. and Sulsky, D. "Snap back overcome by using very high (unrealistic) fracture energy". *Geophysical Research Letter* 35 (L21705).

Mergheim, J., Kuhl, E. and Steinmann, P. (2004). "A hybrid discontinuous Galerkin/interface method for the computational modelling of failure". *Communications in Numerical Methods in Engineering* 20(7), 511–519.

Miehe, C., Hofacker, M. and Welschinger, F. (2010). "A phase field model for rate-independent crack propagation: Robust algorithmic implementation based on operator splits". *Computer Methods in Applied Mechanics and Engineering* 199(4548), 2765 – 2778.

Moes, N., Dolbow, J. and Belytschko T. (1999). "A finite element method for crack growth without remeshing". *International Journal for Numerical Methods in Engineering* 46(1), 131–150.

Ngo, D. and Scordelis, A. (1967). "Finite element analysis of reinforced concrete beams". *ACI Journal* 64:(14), 152163.

Nguyen, C. T., Nguyen, G.D., Nguyen, V. P. and Bui H. (2015a) "Analysis of geomaterial failure using a constitutive modelling approach with an embedded localisation band". *International Journal of Rock Mechanics and Mining Sciences*. Under review.

Nguyen, G. D., Einav, I. and Korsunsky, A.M. (2012). "How to connect two scales of behaviour in constitutive modelling of geomaterials". *Geotechnique Letters* 2(0), 129–134.

Nguyen, G. D., Korsunsky, A.M. and Einav, I. (2014). "A constitutive modelling framework featuring two scales of behaviour: Fundamentals and applications to quasi-brittle failure". *Engineering Fracture Mechanics* 115(0), 221 – 240.

Nguyen, V. P., Nguyen, G.D., Nguyen, C.T. and Shen, L. (2015b). "Continuum constitutive modelling with embedded cohesive behaviour for failure analysis of quasi-brittle materials". *Engineering Fracture Mechanics*. Under revision.

Nguyen, V.P. (2014a). "Discontinuous Galerkin/Extrinsic cohesive zone modeling: implementation caveats and applications in computational fracture mechanics". *Engineering Fracture Mechanics* 128, 37–68.

Nguyen, V.P. (2014b). “An open source program to generate zero-thickness cohesive interface elements.” *Advances in Engineering Software*, 74, 27–39.

Nguyen, V.P., Lloberas Valls, O., Stroeven, M. and L. J. Sluys. (2010). “On the existence of representative volumes for softening quasi-brittle materials-A failure zone averaging scheme”. *Computer Methods in Applied Mechanics and Engineering*, 199(45-48):3028–3038.

París, F., Correa, E. and Mantic, V. (2006). “Kinking of transversal interface cracks between fibre and matrix”. *Journal of Applied Mechanics* 74(4):703–16.

Peerlings, R. H. J., de Borst, R., Brekelmans, W. A. M. and de Wree, J. (1996). “Gradient enhanced damage for quasi brittle materials”. *International Journal for Numerical Methods in Engineering* 39, 3391–3403.

Turon, A., Camanho, P.P., Costa, J. and Dávila, C.G. (2006). “A damage model for the simulation of delamination in advanced composites under variable-mode loading”. *Mechanics of Materials* ;38(11):1072–89.

Rashid, Y. (1968). “Ultimate strength analysis of prestressed concrete pressure vessels”. *Nuclear Engineering and Design* 7(4), 334 – 344.

Wells, G.N., Sluys, L.J., (2001). “A new method for modelling cohesive cracks using finite elements”. *International Journal for Numerical Methods in Engineering* 50, 2667-2682.

Xu, X.-P. and Needleman, A. (1994). “Numerical simulations of fast crack growth in brittle solids”. *Journal of the Mechanics and Physics of Solids* 42, 1397-1434.